MEASUREMENT AND PREDICTION OF TIP LEAKAGE LOSSES IN AN AXIAL-FLOW TRANSONIC TURBINE

M. Wehner
HBI Haerter AG,
8002 - Zurich, Switzerland.

J. Bütikofer
ABB Power Generation Ltd,
5401 - Baden, Switzerland.

C-W. Hustad and A. Bölcs
Swiss Federal Institute of Technology,
EPFL, 1015 - Lausanne, Switzerland.

ABSTRACT

This paper presents a simple method for predicting tip leakage losses in transonic axial-flow turbines. The method is based upon experimental work conducted on a flat plate at 5° incidence and with isentropic exit Mach number of 1.26. The tip gap height was varied from zero up to 15% of chord. Measurements were made (using Laser-2-Focus) of velocity vectors around the tip gap region. These revealed a strong shear layer emerging from the gap onto the suction side of the plate. The relative angle between the leakage flow and the freestream was identified as a key parameter determining the subsequent mixing and overall loss generation. The proposed model applies two-dimensional potential flow analysis to estimate the flow angle as a function of tip gap height and the angle of incidence.

Subsequently, comparisons were made with experimental results obtained in an annular cascade on the outer profile of the last-stage blade of a steam turbine. The predicted tip leakage losses compare favourably with the measured values.

NOMENCLATURE

B	= Span	z	= Spanwise coordinate
C_D	= Discharge coef.	r	= Radius
C_L	= Lift coef. (see Eq.3)	s	= Entropy
M	= Mach number	t	= Blade pitch
M^*	= Laval number, w/a^*	w	= Flow velocity
R	= Gas constant; radius (see Table 1)		
T	= Temperature	α	= Flow angle
Z	= Zweifel coef. (see Eq.4)	α_i	= Incidence angle
c	= Chord length	β	= Flow angle
c_p	= Specific heat	β_g	= Stagger angle
d	= Profile thickness	γ	= Specific heat ratio
h	= Enthalpy	δ	= Separation (see Fig.3)
$\dot{m}$	= Mass flow	ρ	= Density
p	= Static pressure	τ	= Tip gap height
x	= Chordwise coordinate		
y	= Vertical coordinate (normal to x and z)		
a^*	= Critical (M = 1) velocity of sound, $a_o\sqrt{2/(\gamma+1)}$		
β_m	= Mean flow angle, $\tan^{-1}\{(\tan\beta_1+\tan\beta_2)/2\}$		
ζ	= Enthalpy loss coefficient, $(h_2-h_{2s})/(h_o-h_{2s})$		
Y	= Stagnation pressure loss coefficient (see Eq.1)		

Subscripts

*	= Critical (M = 1).	s	= Isentropic
o	= Stagnation	1,2	= Inlet and Outlet
M	= Main flow	N	= Normal to chord line
T	= Parallel with chord line		

INTRODUCTION

In axial-flow gas and steam turbines the necessary tip clearance between the rotor and casing is determined by several factors including blade span, temperature, and cyclic stresses which occur throughout the operating range, especially during the start-up and shut down phases. It is well known that this clearance height is a compromise between safety considerations and stage efficiency. For unshrouded blades it is the blade loading which drives the leakage flow through the gap region. The subsequent roll-up of the leakage vortex leads to a complicated three-dimensional flow structure which is convected downstream through the blade passage. The resulting tip leakage loss attributable to unshrouded blades is a consequence of the inevitable mixing between the leakage flow and the freestream. In addition there is also an underturning of the endwall flow leading to poor alignment with the downstream guide vanes.

An accurate estimate of the tip leakage losses and a knowledge of the most important loss mechanisms, is a key

feature of turbine design. Current prediction models are mostly based on experimental investigations conducted at subsonic—often incompressible—flow conditions. Modern turbomachines operate extensively in the transonic regime, this being particularly so for the first compressor stages and the last stages of the turbine, where blade loading is high. It is not known how accurate established prediction models are when extrapolated to such conditions. The present experimental study of tip leakage flow was therefore undertaken in order to develop an improved model for predicting tip leakage losses in transonic flow.

OVERVIEW OF EXISTING LOSS MODELS

The total-pressure loss coefficient Y is defined as,

$$Y = (p_{o1} - p_{o2})/(p_{o2} - p_2) \tag{1}$$

Tip leakage loss models can be classified into three main categories: those based on momentum considerations; those based on energy considerations; and models which apply a mixing analysis. The first two categories have recently been reviewed in detail by Yaras and Sjolander(1992).

Momentum Based Models

Momentum based models have been presented by Betz(1926), Ainley and Mathieson(1951), Lakshminarayana and Horlock(1965), Dunham and Came(1970), and Lakshminarayana(1970). These generally simulate the tip leakage vortex and determine the induced drag of the vortex on the blade.

The often used method of Ainley and Mathieson results in a loss coefficient,

$$Y_{gap} = K\,(\tau/B)\,C_L^2\,(c/t)^2\,Z \tag{2}$$

with K being 0.5 for unshrouded blades and 0.25 for shrouded blades. The Lift coefficient C_L is defined as,

$$C_L = 2(t/c)(\tan\beta_1 - \tan\beta_2)\cos\beta_m \tag{3}$$

and the Zweifel coefficient is given by,

$$Z = \cos^2\beta_2/\cos^3\beta_m \tag{4}$$

Bammert et al.(1968), in compliance with their own experiments, adapted the equation given by Stodola(1924), and hypothesized that the circumferential component of the tip leakage velocity remained constant, while the absolute value attained the same magnitude as the velocity of the turned flow in the blade row due to the expansion. Under these conditions they determined the tip leakage loss to be given by,

$$\zeta_{gap} = 0.5\,\frac{f_{gap}}{F_{can}}\sqrt{1 + \tan^2\beta_2 - (w_{1x}/w_{2x}\tan\beta_1)^2} \tag{5}$$

where f_{gap} and F_{can} are respectively the annular cross-sections of the gap and the whole passage, while w_{1x} and w_{2x} are the axial components of the flow velocity upstream and downstream of the rotor. The value 0.5 is an empirical correction factor. Experiments on a reduced size low-pressure steam turbine, by Zimmermann and Stetter(1993) showed good agreement with this model.

Energy Based Models

Energy based models (eg. Rains(1954), Vavra(1960)) consider directly the conversion of kinetic energy, and require a prediction of the tip gap mass flow. The kinetic energy of the component normal to the chord is assumed to be lost and constitutes the tip leakage loss.

Yaras and Sjolander(1992) showed that Vavra's model under estimated the losses in comparison to their own measurements, and presumed that this was due to the production of kinetic energy within the gap. They developed an improved model by dividing the tip leakage loss into the kinetic energy loss due to the gap (Y_{gap}) and the internal gap loss ($Y_{gap,int}$). The resulting expressions for these becomes,

$$Y_{gap} = 2\,K_E\,C_D\,(\tau/B)\,C_L^{1.5}\,(c/t)\,Z \tag{6}$$

$$Y_{gap,int} = C\,K_G\,\frac{(c/B)\,C_D\,C_L^{0.5}}{\cos\beta_m}\,(c/t) \tag{7}$$

with $K_E = 0.566$ and $K_G = 0.943$ for a front loaded blade, while 0.5 and 1.0 respectively for a mid-loaded blade. The constant C was estimated to be about 0.007, while C_D is the discharge coefficient through the *vena contracta*.

Models Based on a Mixing Analysis

Storer and Cumpsty(1994) presented an incompressible approach based on a simple model for the mixing of the tip gap flow and the main flow. They observed from Navier-Stokes calculations that the loss creation occurred essentially in the shear layer between the main stream and the tip leakage flow. The respective velocity of these flows was similar, while the relative flow angles differed considerably. They proposed the model shown in Fig.1.

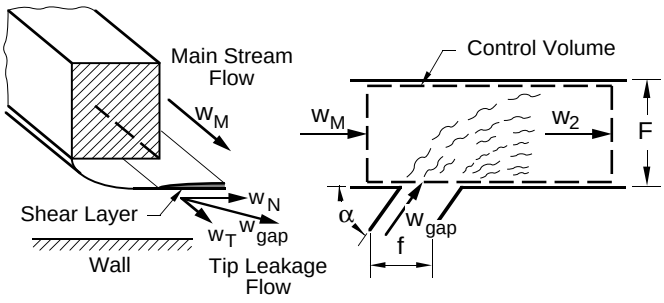

Figure 1: Model for the shear layer at the tip gap exit (left), and the mixing model (right) for tip leakage flow with the main flow, as proposed by Storer and Cumpsty(1994).

Two incompressible flows having equal velocities ($w_M = w_{gap}$) are mixed to a uniform flow with velocity w_2 in a constant cross-section F. The tip leakage flow has a cross-section f and enters the control volume at an angle α relative to the main stream flow. The ratio of the two flow areas is denoted by $\chi = f/F$, which is given by the geometric data of the blade row. Applying conservation of mass and momentum in the main flow direction (but neglecting skin friction) gives the loss coefficient,

$$Y_{gap} = \chi \sin\alpha \left\{ \frac{2 + \chi \sin\alpha - 2\cos\alpha}{(1 + \chi \sin\alpha)^2} \right\} \qquad (8)$$

This approach is an extension of one proposed by Denton and Cumpsty(1987), who assumed a flow angle of $\alpha = 90°$. The area F is given by the span times the staggered blade pitch—the latter being approximated by the pitch times cosine of the stagger angle. The area f is the effective tip gap height times chord. The resulting expression for the area ratio becomes,

$$\chi = \frac{C_D \, \tau \, c}{B \, t \, \cos\beta_g} \qquad (9)$$

where C_D was 0.8. To apply this model the flow angle in the gap has to be estimated. For simplicity Storer and Cumpsty(1994) used a constant value of $\alpha = 50°$, which was obtained from measurements using miniature probes.

Denton(1993) considers entropy as being the essential measure of loss. The entropy of a perfect gas relative to a reference condition is a function of temperature and pressure, so that,

$$s - s_{ref} = c_p \ln\left\{\frac{T}{T_{ref}}\right\} - R \ln\left\{\frac{p}{p_{ref}}\right\} \qquad (10)$$

Here the reference values may be either static or stagnation conditions—by definition this change is isentropic. In adiabatic flow the total temperature remains constant and the entropy rise from inlet to outlet becomes,

$$\Delta s = -R \ln\left\{\frac{p_{02}}{p_{01}}\right\} \qquad (11)$$

For flow in a stator—as well as in a stationary test blade row—the total pressure loss is thus a direct measure of entropy rise.

A general analysis for the direct measure of entropy rise due to mixing of two compressible flows at different total temperature and total pressure, was given by Shapiro(1953). Denton(1993) simplified this analysis to yield,

$$\Delta s = c_p(\gamma - 1)\, M_M^2 \left(\frac{\dot{m}_{gap}}{\dot{m}_M}\right)\left(1 - \frac{w_{gap}\cos\alpha}{w_M}\right) \qquad (12)$$

where $\dot{m}_{gap}$ and $\dot{m}_M$ denote the tip leakage and the main stream mass flow, and M_M is the Mach number of the main flow. This equation is valid for flows with equal total temperature, mixing at constant area or constant pressure, and when one of the mixing flows is relatively small compared to the other. Such conditions are often representative of the tip leakage flow sketched in Fig.1, where the velocities of the main flow and the tip gap flow can be different.

An alternative approach is to consider that the relative kinetic energy of the tip gap flow cannot be recovered and thus represents the tip leakage loss. For the case presented in Fig.1 the entropy rise then becomes,

$$\Delta s = 0.5\, c_p\, (\gamma - 1)\, M_M^2 \left(\frac{\dot{m}_{gap}}{\dot{m}_M}\right) \times \left(\frac{(w_M - w_{gap}\cos\alpha)^2 + (w_{gap}\sin\alpha)^2}{w_M^2}\right) \qquad (13)$$

Equations (12) and (13) are identical when the main-flow velocity equals the tip leakage velocity. For the energy based Eq. (13), increasing tip gap velocity leads to a lower prediction of the losses. Generally the momentum based Eq. (12) is considered to be physically more correct because it allows for static pressure recovery from the momentum of the tip leakage flow.

DEVELOPMENT OF A NEW LOSS MODEL

The proposed tip leakage loss model was developed from experimental work conducted using two different test facilities. The first was a simple flat-plate configuration in a transonic wind tunnel. Here the tip leakage flow could be investigated in detail. The second was an annular cascade with periodic conditions where the tip leakage losses were measured.

Velocity in the Gap of a Flat Plate

Wehner et al.(1996) studied tip clearance effects using three flat plates having 100mm chord, 4mm thickness and rounded leading and trailing edges. The experiments were

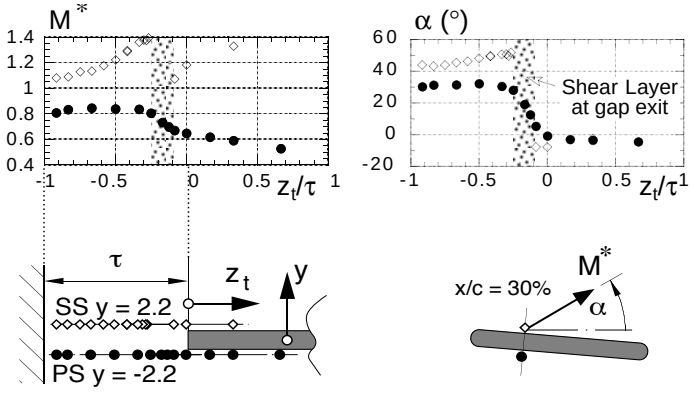

Figure 2: Laval Number and Flow Angle at 30% Chord for $\tau/c = 6\%$. Units bottom left are in mm.

conducted in a 180×100mm transonic working section, with inlet Mach number of 0.56 and isentropic exit Mach number of 1.26. Extensive Laser-2-Focus (L2F) anemometry was used to measure tip gap velocity vectors for gap heights equivalent to 6, 10 and 15% of chord.

The spanwise variation of velocity vectors for the 6% gap (at 30% chord) just above and below the blade, are presented in Fig.2 using Laval number M^* and flow angle α. The bottom left sketch represents a cross section of the blade tip region together with the location of each measurement station. Bottom right sketch shows the blade profile at 5° incidence together with our definition of the flow vector.

Level with the pressure surface (PS) the velocity distribution and flow angle across the gap are comparatively uniform (as shown by the solid circles), although dropping slightly close to the tip. In this region the third velocity component (which could not be measured) induces a significant error. Level with the suction surface (SS) the flow angle and velocity increases when moving from the wall towards the tip. There exists a zone from 10 to 25% of the gap height (from the tip) where it was not possible to measure with the L2F. The flow angle change across this region was about 60°, thus revealing the existence of a strong shear layer.

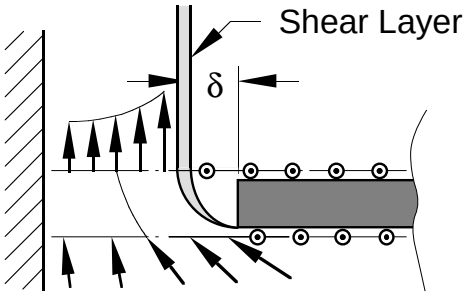

Figure 3: Interpretation of the Conditions at the Tip.

An interpretation of the flow conditions is given in Fig.3. A separation zone develops from the PS corner; it remains detached due to the comparatively larger tip-gap height to blade-thickness ratio. This region develops into a shear layer at the gap outlet(SS), and separates the mainstream flow from the tip leakage flow, at a distance δ from the tip. The magnitude of the flow velocities is similar, and it could be argued that it is equalization of the difference in flow angle which is the main loss producing mechanism, rather than an eventual averaging of the velocities.

Fig.4 shows L2F-measurements from Wehner et al.(1996) which have been plotted against the spanwise coordinate z_t (non-dimensionalized by δ). Datum is at the tip with positive away from the adjacent wall. The flow vector comprises a normal (N) and a tangential (T) component with respect to the chord line. Comparison is made for three tip clearances at 50% chord, and shows that the tangential component of the Laval number M^*_T remains constant over the gap height, while the normal component varies in a significant manner. For all three clearances the curves

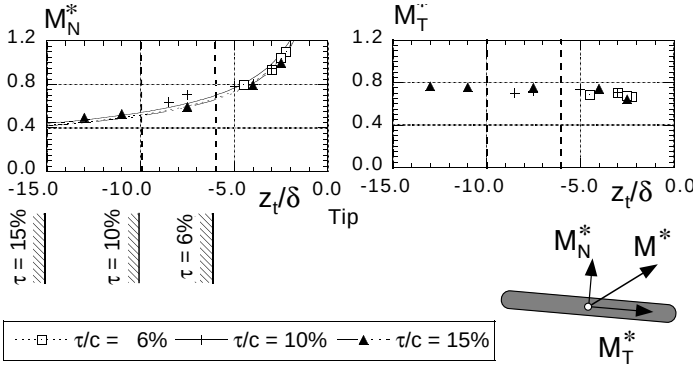

Figure 4: Velocity components in the Gap at 50% Chord.

non-dimensionalize rather well. An approximation to the measured values is given by Eq.(14).

$$M^*_N = \frac{k}{\sqrt{-z_t/\delta}} \; ; \; z_t < 0 \qquad (14)$$

where the coefficient k is determined empirically in order to get the best curve fit as shown in Fig.4 and originally presented by Wehner(1996), who also suggests that the relationship is valid along most of the chord: it is only when approaching the aft part of the blade that noticeable discrepancies appear. Furthermore, there is no indication of a significant boundary layer adjacent to the wall surface. This suggests that primarily high energy fluid from the free stream dominates in the gap.

Loss Measurements in the Annular Cascade

The configuration shown in Fig.5 was investigated in the EPFL annular cascade described by Bölcs(1983). The profile corresponds to a conical cut from the outer section of the last-stage blade in a low pressure steam turbine. Apart from the profiled leading edge region, both surfaces are nearly straight with maximum thickness at 7% chord: this decreases steadily ending in a circular trailing edge. The profile from the real machine had been reduced in size and projected onto a cylindrical cut for the present study. Dimensions of the test configuration is given in Table (1).

Inflow conditions were measured using a 3-hole pitot probe to determine total and static pressure, and pitch angle β_1. The radial yaw angle was also checked and found to be $< \pm 1°$. Measurements were made in the outlet plane us-

c =	75.0	B =	40.0	R_{HUB} =	160.0
d_{max} =	3.0	d_{min} =	1.7	β_g =	65.9°

Table 1: Geometric parameters for the 16 blades in the annular cascade. All lengths are in mm.

ing a 5-hole pitot probe as described by Schulz(1995). This was calibrated over a Mach number range from 0.2 up to 1.72; for yaw-angles of $\pm 22°$; and a pitch variation of $\pm 25°$.

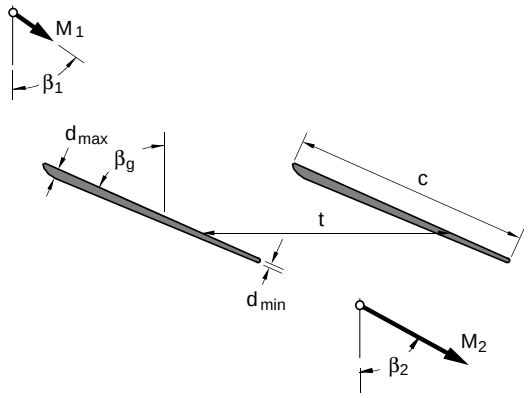

Figure 5: Blade Configuration in the Annular Cascade.

Measurements at the inlet and the outlet plane were used to calculate the mixed-out loss coefficient as described by Dzung(1971). This approach considers conservation of momentum in three directions and transforms the 3D non-homogeneous flow field into a one-dimensional theory applicable to turbomachines.

Basic Concept for the New Loss Model

It is usual to divide the losses into different components which can then be estimated independently and subsequently superposed. In this study we consider the overall loss to comprise of the following terms:

(i) ζ_{BP}, Basic profile loss due to surface friction and separation of the 2D flow on the profile.

(ii) ζ_{TE}, Trailing edge loss due to the finite thickness of the trailing edge.

(iii) ζ_{Shock}, Shock losses due to shock waves which occur in between the blade row.

(iv) ζ_{SEC}, Secondary losses arising due to secondary flow driven by inviscid flow phenomena near the sidewalls (casing and hub).

(v) ζ_{SWF}, Side wall friction loss attributable to hub and casing outside of the blade row.

(vi) ζ_{gap}, Tip gap loss due to the flow around the blade ends.

Combining (i), (ii) and (iii) to define profile loss ζ_{P}, and letting (iv) and (v) be the end loss ζ_{end}, the overall loss can be written as,

$$\zeta = \zeta_{\mathrm{P}} + \zeta_{\mathrm{end}} + \zeta_{\mathrm{gap}} \qquad (15)$$

The assumption for applying Eq.(15) is that the profile and end loss can be obtained at zero clearance; and are independent of variation in gap height. Although this simple but practical approach only partly represents the true conditions, it is often used in the literature (see Vavra(1960), Dunham and Came(1970)).

When increasing gap height, the profile loss is reduced because of the shorter blade span. This was important in the present study due to the rather low tunnel aspect ratio. The secondary losses will reduce with increasing gap height as stated by Yaras and Sjolander(1992). The zero gap loss $\zeta_{\tau=0}$, which combines the profile and secondary loss is therefore weighted by the remaining span so that,

$$\zeta = (1 - \tau/\mathrm{B})\,\zeta_{\tau=0} + \zeta_{\mathrm{gap}} \qquad (16)$$

The profile loss is uniformly distributed over the span and independent of the absolute value of the tunnel width. The end losses and the tip leakage loss are concentrated near the side walls; but when calculating the loss coefficient these are averaged over the width. Thus the values depend upon the aspect ratio.

To simplify use of equation (12) or (13) we need to develop expressions for average flow variables representative of the main flow and tip leakage flow within the gap. The mass flow can be written as,

$$\dot{\mathrm{m}}_{\mathrm{gap}} = \rho_{\mathrm{gap}}\,\mathrm{w}_{\mathrm{gap}}\,\tau\,\mathrm{c}\sin\alpha\,\mathrm{C_D} \qquad (17)$$

$$\dot{\mathrm{m}}_{\mathrm{M}} = \rho_{\mathrm{M}}\,\mathrm{w}_{\mathrm{M}}\,\mathrm{B}\,(\mathrm{t}\,\cos\beta_{\mathrm{g}} - \mathrm{d}) \qquad (18)$$

where $\mathrm{C_D}$ accounts for flow blockage in the gap due to the reduced area following flow separation. The product of span, B, and the bracketed expression in Eq.(18) represents the cross-sectional area of the main flow: for low turning blade rows this is a reasonable approximation. For large gap height the losses within the gap are considered to be relatively low compared to the subsequent mixing losses, and are therefore neglected here. The dominance of high-velocity free-stream fluid within the gap infers that density can, for both flows, be derived from the isentropic relationship based on upstream stagnation conditions. Hence,

$$\rho = \frac{\mathrm{p_{o1}}}{\mathrm{R\,T_o}}\left(1 - \frac{\mathrm{w}^2}{2\,\mathrm{c_p T_o}}\right)^{\frac{1}{\gamma-1}} \qquad (19)$$

The blade pressure distribution at midspan shows only a slight dependence on the tip gap height: near the tip the mean chordwise pressure remains relatively constant with variation of the gap height. Hence the average value of velocity on the suction side is essentially independent of the tip gap size. The mean velocity in the gap is also relatively independent of the tip gap height and is similar to the suction side velocity. For this reason the isentropic velocity at the blade row exit is chosen for the two velocities so that,

$$\mathrm{w_M} = \mathrm{w_{gap}} = \mathrm{w_s} = \sqrt{2\,\mathrm{c_p T_o}\left(1 - (\mathrm{p_2}/\mathrm{p_{o1}})^{\frac{\gamma-1}{\gamma}}\right)} \qquad (20)$$

To apply this model the exact blade profile need not be fixed. Therefore no information regarding blade pressure distribution is necessary. If these are available, then the isentropic suction side velocity, determined by the mean static suction side pressure, can be used instead of the isentropic exit velocity.

Determination of Flow Angle in the Gap

A simple approach based upon incompressible potential flow theory is used to determine the flow angle in the gap. The tip leakage flow may be averaged over the chord and considered as two-dimensional flow around a plate of infinitesimal thickness, as shown in the left of Fig.6.

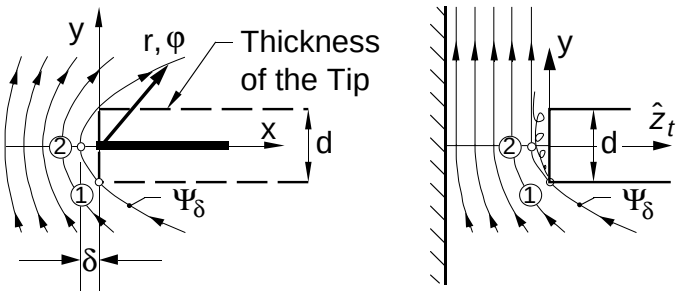

Figure 6: Representation using Potential Flow Theory.

Combining coordinates x and y into a complex variable $z = x + iy$ where $i = \sqrt{-1}$, we write the complex function,

$$F(z) = \Phi(x, y) + i\Psi(x, y) \tag{21}$$

where Φ is the velocity potential and Ψ the stream function. The velocity components are then given by,

$$u = \partial\Psi/\partial y \;\; ; \;\; v = -\partial\Psi/\partial x \tag{22}$$

The case for the so-called flow around a plate of infinitesimal thickness (360° turn), which extends from x equals 0 to ∞, is shown on the left in Fig.6. Applying this approach to conditions at the tip of the blade leads to the model shown in the right of the same figure. On approaching the gap the real flow (see Fig.3) is similar to the theoretical potential flow.

For large gaps, flow separation occurs at the PS corner and remains unattached. We assume that the maximum extension δ of this separation line may be described by the stream line Ψ_δ which just cuts the corner of the blade tip.

Using $z = re^{i\varphi}$ leads to the complex potential F(z) of the corner flow being given by,

$$F(z) = (k/n)r^n\,(\cos n\varphi + i \sin n\varphi) \tag{23}$$

and with n = 1/2 the stream function can be written as,

$$\Psi = 2k\sqrt{r}\sin(\varphi/2) \tag{24}$$

Evaluating the stream function Eq.(24) for the stream line which just touches the corner of the tip at the points marked 1 and 2 in Fig.6, yields the distance to the separation from the tip, giving $\delta = d/4$. The experimental value of δ was estimated for the case shown in Fig.2 to vary over 10 to 25% of gap height from the tip. This is equivalent to between 0.6 and 1.5mm, which would seem to be in accord with the value of 1.0mm based upon the potential flow formulation.

From Eq.(22) we can derive the component of the tip leakage velocity, normal to the chord along the mid-blade plane, to be,

$$w_N = v(\varphi = 180°) = \frac{\partial\Psi}{\partial r} = \frac{k}{\sqrt{r}} \tag{25}$$

As shown by Eq.(14) and in Fig.4 this relationship may be used as a relatively good curve fit for the L2F measurements in the gap. So even if the incompressible potential flow analysis can not describe the detail of the tip leakage flow, the theory can reproduce relatively well the gap conditions in the mid-blade plane.

Integration of Eq.(25) leads to a mean value for the normal velocity in the gap. The normal velocity within the separation zone is small so that integration limits are from the wall to the separation line (ie. $-\tau < z_t < -\delta$). This takes account of a certain reduction in the discharge which is normally attributed to the discharge coefficient, hence $C_D = 1$. Integration of Eq.(25) yields,

$$\overline{w_N} = \frac{2k}{1 + \sqrt{\hat{\tau}}} \tag{26}$$

where $\hat{\tau} = \tau/\delta$. However as inferred by Fig.7 this relationship is only really valid when $\tau \gg \delta$.

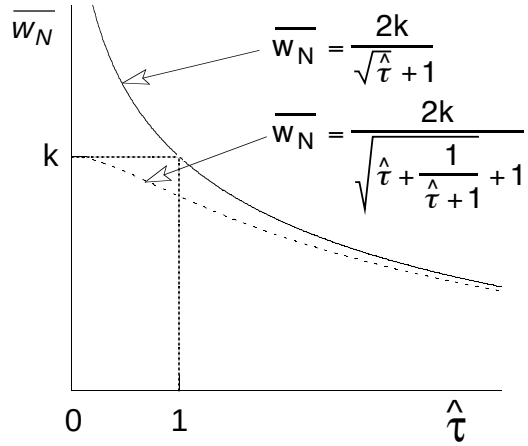

Figure 7: Function for Normal Tip Leakage Velocity.

A more appropriate formulation, which can also be applied to smaller gap heights, is therefore given by Eq.(27). This is also shown for comparison in Fig.7.

$$\overline{w_N} = \frac{2k}{1+\sqrt{\hat{\tau}+\frac{1}{\hat{\tau}+1}}} \qquad (27)$$

The flow angle in the gap is given by the relationship $\alpha = \sin^{-1}\{\overline{w_N}/w_{gap}\}$. For small gaps when $\hat{\tau} \to 0$, the tip gap flow angle $\alpha \to 90°$, so that $\overline{w_N}$ tends to w_{gap} and in accordance with Eq.(27) becomes equivalent to k. Therefore it is reasonable to substitute w_{gap} in place of k.

This leads to the first term in Eq.(28), which expresses the flow angle ($\overline{\alpha}$) as a function of the non-dimensionalised tip gap height ($\hat{\tau}$). A further important influence comes from the incidence angle α_i. With an infinitely large gap, $\overline{\alpha}$ should tend to the incidence angle α_i, while for small gaps α_i should have no influence on the leakage angle $\overline{\alpha}$. This behaviour is expressed by the second term in Eq.(28).

$$\overline{\alpha} = \sin^{-1}\left\{\frac{2}{1+\sqrt{\hat{\tau}+\frac{1}{\hat{\tau}+1}}}\right\} + \alpha_i \frac{\hat{\tau}}{\hat{\tau}+1} \qquad (28)$$

Applying Eq.(28) led to a small under estimation of the tip leakage losses measured in the annular cascade. The flow angle is derived from measurements in the middle of the blade thickness. Between this location and the outlet of the gap there occurs an acceleration of the normal component of the velocity which results in a slightly higher flow angle. This can be taken into consideration by an empirical correction factor $K_N = 1.13$ so that,

$$\alpha = \tan^{-1}\{K_N \tan\overline{\alpha}\} \qquad (29)$$

Fig.8 shows comparisons between this model and measurements taken in the annular cascade with a mean inlet flow angle range $41.6° < \overline{\beta_1} < 60.5°$ and an averaged isentropic exit Mach number range $1.18 < \overline{M_{2is}} < 1.44$.

Both measurements and model are in good agreement and show a non-linear behaviour with varying gap height. The midspan profile loss coefficient is estimated to be $\zeta = 0.025$ for the top left case in Fig.8 and varies between 0.02 and 0.05 for all the cases shown. The tip leakage losses are rather high compared with the profile losses because of the small blade span.

The exit Mach number influences primarily the pressure distribution over the aft part of the suction surface, while the inlet angle has an influence over the whole chord along the pressure side (Wehner, 1996). This leads to a strong dependence of the tip leakage loss on the inlet flow angle while there is almost no influence on the exit Mach number.

CONCLUSIONS

The proposed tip leakage loss model for transonic axial-flow turbine blade rows is based on a mixing analysis originally formulated by Shapiro(1953) with simplifications given by Denton(1993). The gap and main flow quantities are estimated using a simple potential flow model which is derived from Laser-2-Focus measurements within the gap of a flat plate.

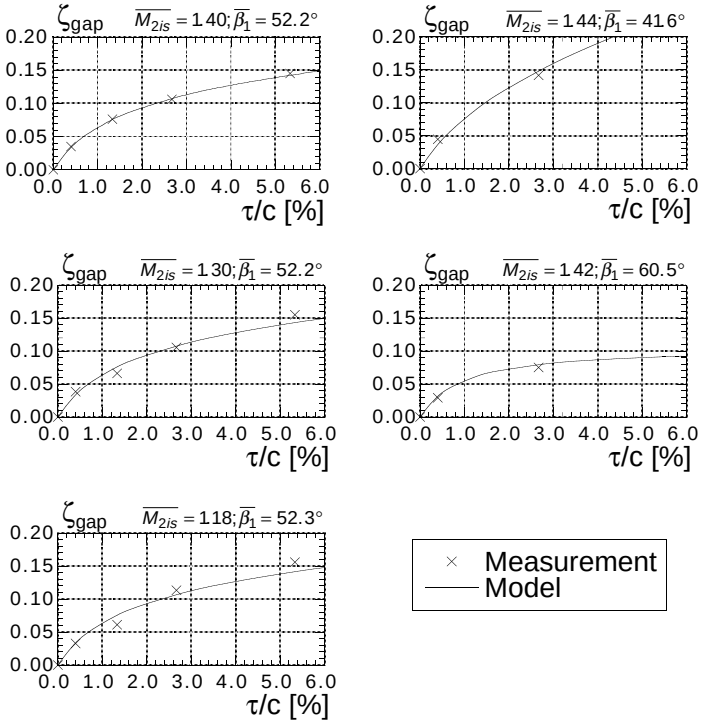

Figure 8: Comparison between Measured and Predicted Tip Leakage Losses in the Annular Cascade.

The model has been calibrated against loss measurements made in a non-rotating annular cascade having periodic flow conditions. It should be valid for transonic blade profiles which are thin, have low curvature, and fall within the range of tip clearances which are typical for the blades of a steam turbine last stage.

For smaller gaps, as used in gas turbines, internal gap losses and influence of the wall boundary layer—which are not modelled here—will have an increasing influence on the tip leakage loss. Therefore the applicability of this model for such a range of tip clearance has yet to be confirmed.

We have not investigated the influence of relative wall motion nor tip profile geometry, however such work is in progress (Hustad et al.,1997).

ACKNOWLEDGEMENTS

Financial support for this project was provided by the Swiss goverment through the "Nationaler Energie-Forschungs-Fonds" (NEFF) and by ABB Power Generation Ltd., Baden, Switzerland.

REFERENCES

Ainley D. G., Mathieson G. C. R., 1951, "A Method of Performance Estimation for Axial-Flow Turbines", Aeronautical Research Council R&M No.2974.

Bammert K., Klukens H., Hartmann D., 1968, "Der Einflus des radialen Schaufelspalts auf den Wirkungsgrad mehrstufiger Turbinen", VDI-Z. 110, Nr.10.

Betz A., 1926, "Über die Vorgänge an den Schaufelenden von Kaplan-Turbinen", in Hydraulische Probleme, Hrsg.: VDI Verlag, Berlin.

Bölcs A., 1983, "A Test Facility for the Investigation of Steady and Unsteady Transonic Flows in Annular Cascades", ASME-Paper 83-GT-34.

Booth T. C., Dodge P. R., Hepworth H. K., 1982, "Rotor-Tip Leakage: Part I - Basic Methodology", ASME Journal of Engineering for Power, Vol.104, pp.154-161.

Denton J. D., Cumpsty N. A., 1987, "Loss Mechanisms In Turbomachines", Proc. Inst. Mech. Engrs., Cambridge, 1-3 Sept. pp.1-14.

Denton J.D., 1993, "Loss Mechanisms In Turbomachines", ASME Journal of Turbomachinery, Vol.115, pp.621-656.

Dunham J., Came P. M., 1970, "Improvements to the Ainley-Mathieson Method of Turbine Performance Prediction", ASME Journal of Engineering for Power, Vol.92, pp.252-256.

Dzung L.S., 1971, "Consistent Mean Values for Compressible Media in the Theory of Turbomachines", Brown Boveri Rev., Nr.10, pp.485-492.

Hustad C-W., Bölcs A., Wehner M., 1997, "Investigation of Tip Leakage Effects in Transonic Flow Using a Parallel Unstructured Navier-Stokes Code", To be presented, ASME Conference, Orlando, Florida.

Lakshminarayana B., 1970, "Methods of Predicting the Tip Clearance Effects in Axial Flow Turbomachinery", ASME Journal of Basic Engineering, pp.467-482

Lakshminarayana B., Horlock J. H., 1965, "Leakage and Secondary Flows in Compressor Cascades", Aeronautical Research Council R&M No.3483.

Rains D. A., 1954, "Tip Clearance Flows in Axial Flow Compressors and Pumps", California Institute of Technology, Hydrodynamics and Mechanical Engineering Laboratories, Report No.5.

Schulz K., Bölcs A., Dalbert P., 1995, Experimental Investigation in Annular Compressor Cascades at Transonic Flow Conditions", ASME-Paper 95-GT-83.

Shapiro A. H., 1953, "The Dynamics and Thermodynamics of Compressible Fluid Flow", Vol.1, Wiley, New York.

Stodola A., 1924, "Dampf- und Gasturbinen", Springer-Verlag, Berlin.

Storer J.A., Cumpsty N.A., 1994, "An Approximate Analysis And Prediction Method For Tip Clearance Loss In Axial Compressors", ASME Journal of Turbomachinery, Vol.116, pp.648-656.

Vavra M. H., 1960, "Aero-Thermodynamics and Flow in Turbomachines", John Wiley & Sons, New York.

Yaras M.I, Sjolander S.A., 1990, "Development of the Tip-Leakage Flow Downstream of a Planar Cascade of Turbine Blades: Vorticity Field", ASME Journal of Turbomachinery, Vol.112, pp.609-617.

Yaras M.I., Sjolander S.A., 1992, "Prediction of Tip-Leakage Losses in Axial Turbines", ASME Journal of Turbomachinery, Vol.114, pp.204-210.

Wehner M., 1996, "Experimentelle und theoretische Untersuchung der Spaltströmung in einer Turbine bei Überschallabströmung", Ph.D. Thesis. EPFL, Switzerland.

Wehner M., Bölcs A., Bütikofer J., 1996, "Experimental Study of Tip Clearance under Transonic Flow Conditions", ASME-Paper 96-GT-99.

Zimmermann C., Stetter H., 1993, "Experimental Determination of the Flow Field in the Tip Region of a LP-Steam Turbine", ASME-Paper 93-GT-106.